Analysis of Eshelby-Cheng's and Hudson on synthetic cracked models

Jessica P. Henriques [a], Jose J. S. de Figueiredo [a,b], Daniel Leal Macedo [a], Leo Kirchhof Santos [a], Icaro Coutinho [a], Carolina B. da Silva [a], Alberto L. Melo [a] , Mykel Sousa [a] and Felipe Louzeiro [a]
[a]UFPA, Faculty of Geophysics, Laboratory of Petrophysics and Rock Physics–Dr. Om Prakash Verma, Belém, PA, Brazil.
[b]National Institute for Petroleum Geophysics (INCT-GP), Brazil

Abstract

Physical modeling of cracked/fractured media through downscaled laboratory experiments has worked as a great alternative for understanding the effect of anisotropy in the hydrocarbon reservoir, and in the crustal and mantle seismology. The main goal of this work was to experimentally verify the predictions of effective elastic parameters in anisotropic cracked media predicted by Hudson and Eshelby-Cheng's effective cracked models. For this proposal, we carried out ultrasonic measurements on synthetic anisotropic samples with low crack density and different aspect ratios. Six samples were prepared with 5% of crack density. These samples, with three-different aspect ratio cracks (0.13, 0.17 and 0.26), were simulated by penny-shape rubber inclusions in a homogeneous isotropic matrix made with epoxy resin. Moreover, an isotropic sample for reference was constructed with epoxy resin only. Among all samples, three presented only one aspect ratio type (samples with single crack aspect ratio), while other three showed three types of different aspect ratio (mixed crack aspect ratio samples). Regarding predictions performed by the theoretical models, Eshelby-Cheng shows a better fit when compared to the experimental results for samples with single and mix crack aspect ratio. Our comparisons were also performed in terms of γ parameter (Thomsen parameters).

Introduction

Due to the complexity exhibit by the anisotropic rock, even on subsurface, in the mantle or/in the uppermost crust, forward modeling by numerical and physical approaches have been used as an important tool to better understanding the anisotropic phenomenon in these formations [Crampin, 1984a; Shearer, 1988; Crampin, 1986b]. However, most of the times, numerical modeling shows numerical dispersion problems that can be found in the modeling of cracks and fractures [Coates and Schoenberg, 1995; Zhang, 2005]. What is usually done is the replacement of the cracks and fractures by an effective medium in which the individual effects of fractures or cracks cannot be studied [Saenger and Shapiro, 2002]. Using physical modeling, the answer to the numerical ambiguous is not found, since cracks and fractures can be physically simulated by materials having a very low shear modulus (e.g., rubber discs or void spaces) with different physical characteristics [Assad et al. 1992, 1996, 2005; Rathore et al., 1995; Tillotson et al., 2011; Stewart et al., 2013].

Anisotropic modeling through downscaled physical experiments is an alternative for better understanding how cracked media behaves when elastic waves propagate through them. This alternative is acceptable because, in the laboratory, measurements modeling conditions present in the field [De Figueiredo et al., 2013]. Several recent works emphasize the importance of anisotropic physical modeling in exploration geophysics. Assad et al. [1992, 1996] constructed anisotropic samples made with rubber penny-shaped inclusions with different crack densities in an epoxy resin matrix. In this work, it was experimentally verified that the linear relation between the crack density and the Thomsen's parameter (γ), predicted by Hudson's [1981] effective cracked model, is valid for fractured medium with crack density lower than 7%. Based on the same methodology developed by Assad et al. [1992] to construct anisotropic samples, De Figueiredo et al. [2012] and Santos et al. [2015] constructed an anisotropic sample with strip cracks positioned in different orientations for different fracture swarms. They showed the importance of S-wave birefringence to find the fracture preferential direction in fractured media with different fracture orientations.

Rathore et al. [1995] performed a remarkable experiment in physical modeling. Using P and S-wave measurements in manufactured anisotropic dry samples made by penny-shaped void cracks in sand-epoxy matrix, they experimentally tested Hudson [1980,1981] and Thomsen's [1995] cracked models for anisotropic media in saturated conditions. The methodology developed by Rathore et al. [1995] to prepare anisotropic cracked sample have been used by other authors [Tillotson et al., 2012, 2013; Amalokwu, et al., 2015] to construct anisotropic sample, validate other theories or investigate different phenomena regarding elastic wave propagation in fractured media.

As mentioned above, the synthetic anisotropic models constructed (in controlled conditions) by Assad et al. [1992, 1996] and Rathore et al. [1995] were used to validate effective cracked theories such as Hudson [1980, 1981] and Thomsen [1995]. In all these works, it was guaranteed that the wavelength was greater than the dimensions of individual cracks and their separation distance, which is the basis of any effective theory. Other important features in these works were the single aspect ratio cracks in each sample (homogeneity) and cracks with lower aspect ratio. For fractured media with arbitrary aspect ratio cracks, Eshelby [1957] and Cheng [1993],

proposed a model for estimation of effective elastic parameters. Cheng [1993], based on the Eshelby [1957] work, also proposed an effective modulus in an elastic solid with ellipsoidal inclusion that resembles Hudson [1981], but with different considerations. This is a generalization of Hudson's [1981] theory in view of Eshelby-Cheng's [1993] model. There is no limitation about crack aspect ratio. To investigate the effective cracked model of Eshelby-Cheng [1993] and Hudson's [1981] models for cracked sample with different crack aspect ratio is the main purpose of this work.

For this study, we constructed six cracked samples and one uncracked sample as reference. The cracks were simulated physically with penny-shaped rubber inclusions. Three different cracks aspect ratio were used in the cracked samples. The samples were 5% of crack density and were divided in two sub groups that have same crack density but different crack aspect ratio. These sub groups were called single (single aspect ratio cracks) and mix (sample with differents crack aspect ratio) cracked samples. S- wave records were measured as function of the angle of incidence. These wave records were used to estimate the velocities and Thomsen's parameter (γ).

Finally, comparisons between our experimental results and the theoretical predictions by the effective models of Hudson [1981] and Eshelby-Cheng [1993] were performed. Our comparisons were also performed in terms of γ parameters. Considering the fact that, in practice, the anisotropy parameters are difficult to estimate, these estimations based on effective cracked model can be exploited to facilitate seismic anisotropy interpretations using data from seismic (well logs and VSP) and seismology (earthquakes or seisms).

Experimental Procedure

The construction of the cracked samples, as well as the ultrasonic measurements, was carried out at the Laboratory of Petrophysics and Rock Physics-Dr. Om Prakash Verma (LPRP), at the Federal University of Pará, Brazil. Under controlled conditions, six cracked samples were constructed with crack density of 5% and cracks in the sample had different aspect ratio. An isotropic uncracked sample (SFC4) was constructed for reference. Pictures of all samples are depicted in Figure 1.

Sample preparation

The uncracked sample (SFC4) consisted of a single cast of epoxy resin. Samples CF3 to CF8 contained cracks aligned along the Y and X directions and had 5% crack density. All cracked samples were constituted one layer at a time, alternating with the introduction of rubber cracks. To reduce possible boundary effects to a minimum, time interval between the creations of separate layers was kept as short as possible. A constant layer thickness (0.7 cm) was ensured by using the same volume of epoxy resin poured for each layer. Each cracked sample had 7 layers. The solid rubber material used to simulate the cracks in all samples was silicone rubber.

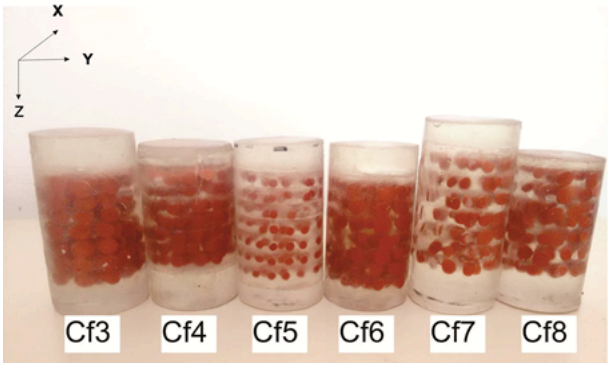

Figure 1. Photograph of the cracked samples with 5% crack density.

As mentioned before, the additional contributions of this work, beyond comparing the theoretical predictions (from different approaches [Hudson, 1981; Eshelby-Cheng, 1993]) with experimental results, was also to verify how single and mixed cracks aspect ratio distribution affects S-wave responses. For this proposal, samples from CF6 to CF8 had cracks with mixed aspect ratio. It is worthy to mention that all crack samples contain oriented cracks with random distribution in the layers. Consequently, this preferential orientation leads to the simulation of a transversely isotropic medium. The HTI media is viewed from above the XZ plane, and VTI from above XY plane (see Figure 1).

The physical and geometrical parameters of the included rubber cracks in each sample are displayed on Table 1.

Table 1. Physical parameters of uncracked and cracked samples and description of each samples based on aspect ratio. The precision of length measurements were about 0.02 cm

Sample Name	Type of crack (crack diameter - %)			Crack Aspect ratio	Length (Y)	Diameter (Z)	Density
	0.6 (mm)	0.45 (mm)	0.3 (mm)		(cm)	(cm)	(kg/cm³)
SFC4	0	0	0	-	7.551	3.598	1239.5
CF3	100	0	0	0.1333	6.81	3.707	1233.7
CF4	0	100	0	0.1778	6.399	3.705	1208.5
CF5	0	0	100	0.2667	6.556	3.616	1307.3
CF6	50	30	20	0.1733	6.538	3.646	1216.7
CF7	40	40	20	0.1778	7.518	3.627	1236.8
CF8	30	50	20	0.1822	6.579	3.742	1182.6

Ultrasonic measurements

The ultrasonic measurements were performed using the Ultrasonic Research System at LPRF with the pulse transmission technique. The sampling rate per channel for all measures of S-wave records was 0.1 μs. The system is formed by a pulse-receiver 5072PR and a pre-amplifier 5660B from Olympus, a USB oscilloscope of 50

MHz from Handscope and S-wave transducers of 1 MHz also from Olympus.

Figure 2 shows the device developed for recording S-wave seismograms, with rotating polarization. The source and receiver transducers were arranged on opposing sides of the samples, separated by the length of the sample measured (Table 1). To ensure that the propagation of the wave was in the desired region of the samples, the transducers were placed at the center of either side. This was made for both wave modes of propagation.

For shear wave, the measurements were realized along the Y direction, being the initial polarization parallel to the cracks (direction X), in XZ plane (see Figure 3b and 3d). We performed measures every 15° until polarization was again parallel to the crack planes (180°). Thirteen traces of S-wave were recorded in each sample.

To estimate P-wave velocities, we used the relation given as

$$V_P(\theta) = \frac{L_P}{t_p(\theta) - \Delta t_p^{delay}}, \quad (7)$$

where Lp is the distance of P-wave propagation, $tp(\theta)$ is the transmission time as a function of the angle with respect to Z-axis of a P-wave and Δt^{p}_{delay} is the delay time due to the P-wave transducers. For P-wave traces recording $\theta=0^{o}$ (propagation in Z axis) and $\theta=90^{o}$ (propagation in X axis).

For S-wave velocities, the equation is similar to P-wave. They are given by

$$V_S(\phi) = \frac{L_S}{t_s(\phi) - \Delta t_s^{delay}}, \quad (8)$$

where Ls is the distance of S-wave propagation, $t_S(\phi)$ is the transmission travel time as a function of the angle with respect to X-axis of S-wave propagations and Δt^{s}_{delay} is the delay time due to the S-wave transducers. The polarization of ϕ=0° and ϕ=180° correspond to the fast S-wave (S_1) and ϕ=90° corresponds to the slow S-wave (S_2).

In this work, we are using the notation for γ, as a function of velocities, as described by Thomsen [1986] as,

$$\gamma = \frac{V_{s1}^2 - V_{s2}^2}{2V_{s2}^2} \quad (9)$$

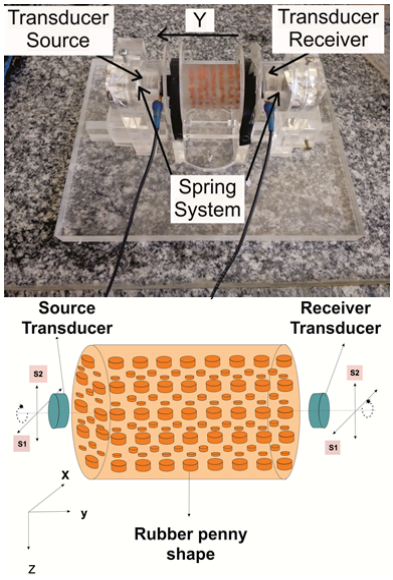

Figure 2. Device developed for S-wave polarization rotation and velocity measurements and sketch of experiment used for S-wave seismogram records

In order to ensure the replicability of the ultrasonic recordings for all samples, it was preserved the same physical condition of the complete electronic apparatus. Furthermore, a holder with spring attached, guaranteed the same coupling between transducer and samples (see Figure 2) and a very slim layer of natural honey was placed at the surface of the samples to establish good contact between transducer and samples.

Experimental results

The results of ultrasonic measures are the traveltime of the waves. With this traveltime, the first arrival was selected. The time delay of S-wave transducers (0.14 μs) was subtracted from the waveforms traveltimes, respectively. With the information of lengths, velocities were calculated. We calculated: S-wave velocities and Thomsen's parameter (γ) for all cracked samples, considering the possible errors due to measurements of length (margin of error = ±0.02 cm) and time travel picking (margin of error = ±0.02 μs).

Shear wave (S) velocities

S-waveforms were measured in the cracked samples, as well as in the isotropic reference model. For all S-wave seismograms, the wave propagation was along to the Y direction. Figure 3 shows the recorded S-wave transmission seismograms for propagation in the Y direction as a function of the angle of S-wave polarization of isotropic sample. As expected, the seismograms recorded in the reference model show uniform first arrivals for all rotations of the polarization angle. All the seismograms are functions of the polarization angle (in the plane XY) for S-wave propagation in the Y direction as recorded in the reference sample (due to the high frequency noise from environment) and also show a visible shear.

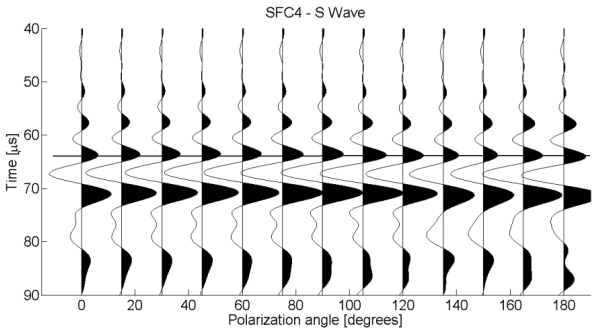

Figure 3. S-wave seismograms as a function of change in polarization from 0° to 180° for propagation in the Y direction in the reference sample (SFC4).

For a better understanding of the two separate peaks we applied, in most samples, a band-pass filter of 40–70–130–160 kHz (perfect pass between 50 and 170 kHz, when the center of filter are in 100 kHz, with linear cut-off ramps in the ranges 20–40 kHz and 130–200 kHz). The cut-off frequency of 160 kHz approximately coincides with the end of the first peak. The result obtained from the difference between the original and filtered seismograms is depicted in Figure 4.

Samples with cracks show the separation of the two different S waves (S_1 and S_2) as we can notice in Figure 4. In order to calculateVs_1 and Vs_2 , it was necessary to select the first arrival in 0° (S_1) and the first arrival in 90° (S_2), as well as the dimensions of each sample (exposed in Table 1). Thomsen's parameter γ was calculated. The margin of errors for S-wave velocities estimative ranged from ± 7.07 m/s to ± 13.68 m/s.

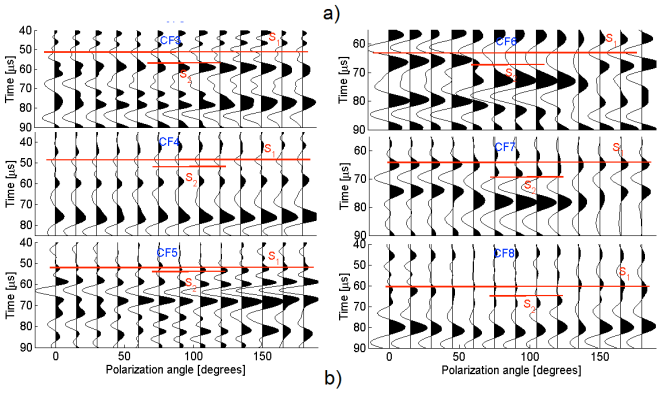

Figure 4. Filtered S-wave seismograms as a function of change in polarization from 0° to 180° for propagation in Y direction and in the samples with 5% crack density.

Table 2. Shear wave velocities VS1 and VS2 in γ direction.

Sample Name	Aspect ratio	Vs_1 (m/s)	Vs_2 (m/s)
SFC4	-	1306.60	1306.60
CF3	0.1333	1337.13	1202.76
CF4	0.1778	1322.65	1222.12
CF5	0.2667	1264.17	1217.23
CF6	0.1733	1196.1	1109.5
CF7	0.1778	1174.50	1088.93
CF8	0.1822	1244.1	1157.1

As observed by Anderson et al. [1974] in theoretical predictions based on Eshelby [1957] model, our V_{S2} velocity is more sensitive to crack aspect ratio/crack density than V_{S1} velocity. In case of mix velocity V_{S2} seems to be much more sensitive to the concentration of adding of cracks with large crack aspect ratios. In other words, it appears that the variations on velocities due to mix crack aspect ratios induce a non-linear behavior on velocities.

Thomsen's parameters

Thomsen's [1986] parameter γ is directly related to the ratio between the t_{S2} and t_{S1} traveltimes which are the highest and lowest S-wave travel times in this fractured medium, respectively. For computing this parameter, it is necessary to have the velocities of S- wave. Figure 5 shows Thomsen's parameter calculated for each model predictions. Predictions by Hudson's [1981] and Eshelby-Cheng's [1993] models show the opposite behaviors between them: while Hudson [1981] increases with aspect ratio, Eshelby-Cheng [1993] decreases with it. As it can be noted, Eshelby-Cheng's [1993] predictions show a best fit with the experimental results. The estimative error for γ parameter is from ±2.36% to ±3.2%.

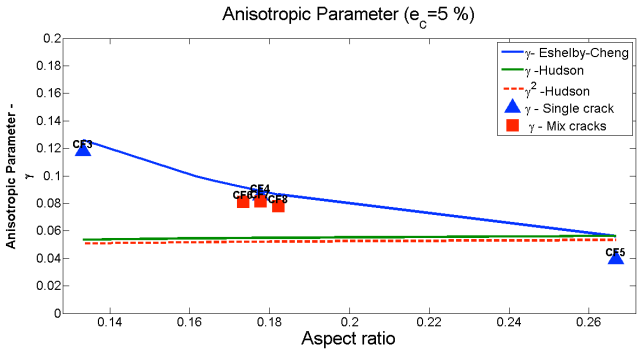

Figure 5. Thomsen's parameter γ as function of aspect ratio for 5% crack density.

Regarding mix samples, as expected, the measured Thomsen's parameters values found were close to the value of the sample, with unique aspect ratio of 0.17 and a better theoretical prediction also occurring for Eshelby-Cheng' [1993] model. A linear decreasing with increasing aspect ratio (small perturbation) can be noted for γ parameters.

5. Discussion and Conclusions

We performed an experimental work based on the construction of synthetic cracked media samples and measurements of elastic ultrasonic waves on these samples. We correlated our experimental results with predictions of two different effective cracked models [Hudson, 1981; Eshelby-Cheng, 1993]. From a direct inspection of S-wave anisotropic parameters, we can observe that Eshelby-Cheng's [1993] model results provided a best fitting between experimental and theoretical results. In past or current literature, there is no experimental work comparing predictions by Hudson, [1981] and Eshelby-Cheng, [1993] models. On the experimental work of Assad et al. [1996], we can notice that the anisotropic parameter γ decreases with increasing of crack aspect ratio for crack densities of 1% and 5%. As we noted on this work, and also by Assad et al. [1996], the increase of crack density overcomes the effect of crack aspect ratio. In other words, the increasing of Thomsen's parameters occurs while crack density increases.

Using the results of Eshelby [1957] to calculate elastic velocities, and consequently the elastic constants of isotropic matrix containing oriented ellipsoidal cracks, Anderson et al. [1974] verified an increasing of elastic velocities (V_{P90} and V_{S1}) with an increase of crack aspect ratio. From other theoretical point of view, Douma [1988] observed those predictions by effective cracked models from Nishizawa [1982] and Crampin [1984b] that the all P and S-wave velocities decrease with increasing of crack-aspect ratio for crack saturated and dry condition.

It is important to mention that the physical reason for difference between Nishizawa [1982] and Crampin's [1984b] models from Eshelby-Cheng's [1993] model predictions for velocities trends (in which they show opposite behavior) should be, in our case, that the cracks are diluted (isolated) in the isotropic background and that there is no contact among them. Other important fact, that can influence in discrepancies of results and theoretical predictions of Douma [1988], is the type of crack filling. We applied the Eshelby-Cheng [1993] and Hudson's [1981] models for cracks filled with weak material, while Douma [1988] applied the Nishizawa [1982] and Crampin's [1984b] models for dry and saturated cracks.

Regarding the results of mix aspect ratio crack samples, it is important to emphasize that, even though our samples are artificial and do not resemble a real rock, we are the first, in a specialized literature, to perform ultrasonic measurements in samples with heterogeneous crack aspect ratio distribution. Obviously, other works using synthetic rocks made by sand and resin gave important contributions on the study of different behaviors of anisotropic media under dry and saturated conditions [e.g., Rathore et al., 1995; Tillotson et al., 2012, 2013; Amalokwu, et al., 2015]. However, none of them verified the influence of variable crack aspect ratio on the anisotropic parameters or behavior. Our samples with mix crack aspect ratio although does not correspond to real rock samples, allow us to verify that small perturbations on the dominant crack aspect ratio of sample can induce significant linear changes in effective elastic parameters of samples. In other words, this small perturbation does not mean a small change in anisotropic parameters.

The rubber inclusions used in this work, simulated ideal ellipsoidal cracks consisting of weak material showing a low shear modulus when compared to the solid resin matrix. Our experiments used an idealized fracture system exhibiting aligned and isolated crack distributions with aspect ratio. The size of the individual cracks was too small when compared with seismic wavelengths. In general context, our results and the results from theoretical predictions [Hudson, 1981; Eshelby-Cheng, 1993], show a stronger dependence on the geometric properties of the cracks than on the weak filling material.

Based on our results, the following observations can be made:

- The decrease in anisotropic parameters γ was observed for both experimental and Eshelby-Cheng's [1993] model prediction as the aspect model ratio increased. This behavior was contrary to the one exhibited by Hudson's [1981] model. The best fit between the experimental and theoretical predictions occurred on Eshelby-Cheng's [1993] model.
- The results related to mix samples show that small perturbations in dominant crack aspect ratio induces a considerable linear change in γ parameters.
- In general, for samples with mixed crack aspect ratio, the theoretical prediction was best performed by Eshelby-Cheng [1993] mode.

Acknowledgements

The authors would like to thank PET/ME-GEOFÏSICA DA CAPES, CNPq (grant number: 459063/2014-6) and PROPESP-UFPA for financial support.

References

Anderson, D.L., Minster, B. and Cole D. (1974). The effect of oriented cracks on seismic velocities*, J. Geophys. Res*., 79, 4011-4015.

Amalokwu, K., Mark Chapman, Angus I. Best, Jeremy Sothcott, Timothy A. Minshull and Xiang-Yang Li. (2015), Experimental observation of water saturation effects on shear wave splitting in synthetic rock with fractures aligned at oblique angles, *Geophysical Journal International*, 200, 17-24.

Assad, J. M. (2005), The effect of orthorhombic anisotropy and its implication for oil recovery and reservoir exploitation, *Geophys. Prospect*., 53, 121–129.

Assad, J. M., R. H. Tatham, and J. A. McDonald (1992), A physical model study of microcrack-induced anisotropy, *Geophysics*, 57, 1562–1570.

Assad, J. M., J. A. McDonald, R. H. Tatham, and Kusky, T. M. (1996), Elas- tic wave propagation in a medium containing oriented inclusions with a changing aspect ratio: A physical model study, *Geophys. J. Int.*, 125(1), 163–172.

Cheng, C. H. (1993), Crack models for a transversely anisotropic medium. *J. Geophys. Res.*, v. 98, p. 675–684.

Coates, R. T and Schoenberg M. (1995), Finite-difference modeling of faults and fractures. *Geophysics*, v. 60, p.1514–1526.

Crampin, S. (1984a), An introduction to wave propagation in anisotropic media. *Geophys. J. Roy. Astr. Soc.*,76, 17-28.

Crampin, S. (1984b), Effective anisotropic elastic constants for wave propagation through cracked solids. *Geophys. J. Roy. Astr. Soc.*, 76, 135-145.

Crampin, S., McGonigle, R., and Ando, M. (1986). Extensive-dilatancy anisotropy beneath Mount Hood, Oregon and the effect of aspect ratio on seismic velocities through aligned cracks. *Journal Geophys. Res.* 91, 12,703-12,710.

De Figueiredo, J. J. S., J. Schleicher, R. R. Stewart and N. Dyaur (2012), Estimating fracture orientation from elastic-wave propagation. *Journal of geophysical research*, v. 117, p. 1-13.

De Figueiredo, J. J. S., J. Schleicher, R. R. Stewart, N. Dyaur, O. Omoboya, R. Wiley and A. William (2013), Shear wave anisotropy from aligned inclusions: ultrasonic frequency dependence of velocity and attenuation. *Geophys. J. Int.*, v. 193, p. 475–488.

Douma, J. (1988), The effect of aspect ratio on crack-induced anisotropy:*Geophysical Prospecting*, 36, 614–632

Eshelby, J. D. (1957), The determination of the elastic field of an ellipsoidal inclusion, and related problems. *Proc. Royal Soc. London A*, v. 241, p. 376–396.

Hudson, J. A. (1981), Wave speeds and attenuation of elastic waves in material containing cracks. *Geophys. J. R. Astron. Soc.*, v. 64, p. 133-150.

Hudson, J. A. and Liu, E. (1999), Effective elastic properties of heavily faulted structures. *Geophysics*, v. 64, n. 2, p.479-489.

Nishizawa, O. (1982). Seismic velocity anisotropy in a medium containing oriented cracks—transversely isotropic case. *Journal of Phys. Earth* 30, 331-347.

Rathore, J. S, Fjaer, E., Holt and R. M., Renlie,. L. (1995), P- and S- wave anisotropy of a synthetic sandstone with controlled crack geometry. *Geophys. Prospect.*, v. 43, p. 711–728.

Saenger, E. H. and Shapiro, S. A. (2002), Effective velocities in fractured media: a numerical study using the rotated staggered finite-difference grid. *Geophysical Prospecting*, v. 50, p.183–194.

Santos, L. K., J.J.S. de Figueiredo, Bode Omoboya, Jörg Schleicher, Robert R. Stewart, Dyaur N. (2015), On the source-frequency dependence of fracture-orientation estimates from shear-wave transmission experiments,. *Journal of Applied Geophysics*, v. 114, p.81-100.

Thomsen, L. (1986), Weak elastic anisotropy. *Geophys.*, v. 51, p. 1954–1966.

Thomsen, L. (1995), Elastic anisotropy due to aligned cracks in porous rock. *Geophysical Prospecting* 43, 805–829.

Tillotson, P., Chapman, M., Best, A.I., Sothcott, J., McCann, C., Shangxu, W. and Li, X. (2011), Observations of fluid - dependent shear-wave splitting in synthetic porous rocks with aligned penny-shaped fractures, *Geophys. Prospect.*, 59(1), 111–119.

Tillotson, P., J. Sothcott, A. I. Best, M. Chapman, and X.-Y. Li (2012), Experimental verification of the fracture density and shear-wave splitting relationship using synthetic silica cemented sandstones with a controlled fracture geometry, *Geophys. Prospect.*, 60, 516–525.

Zhang, J. (2005) . Elastic wave modeling in fractured media with an explicit approach, *Geophysics,* 70, T75–T85.